Available online at www.sciencedirect.com
SCIENCE DIRECT®
Journal of Photochemistry and Photobiology A: Chemistry 170 (2005) 181–188
Journal of Photochemistry and Photobiology A:Chemistry
www.elsevier.com/locate/jphotochem

New fluorescent benzo[*b*]thienyl amino acid derivatives based on sulfanylphenyl benzo[*b*]thiophenes

Mariano Venanzi[a,*], Gianfranco Bocchinfuso[a], Antonio Palleschi[a], Ana S. Abreu[b], Paula M.T. Ferreira[b], Maria-João R.P. Queiroz[b]

[a] *Dipartimento di Scienze e Tecnologie Chimiche, Universita' di Tor Vergata, via della Ricerca Scientifica, 00133 Rome, Italy*
[b] *Departamento de Química, Universidade do Minho, Campus de Gualtar, 4710-057 Braga, Portugal*

Received 19 March 2004; received in revised form 30 July 2004; accepted 6 August 2004

Abstract

Fluorescent derivatives of benzo[*b*]thiophene were synthesized by C–C and C–N palladium catalysed cross-couplings of bromobenzenes with 3-(benzo[*b*]thienyl)boronic acid and bromo- or aminobenzenes with 7-amino or 7-bromobenzo[*b*]thiophene, respectively. The photophysical behaviour of the coupled compounds was investigated in acetonitrile, showing that a delicate balance between the delocalization of the electronic distribution over the entire molecule and the extent of intramolecular charge transfer interactions controls the excited-state relaxation pathway. Some of the new benzo[*b*]thiophene derivatives were linked to the β-carbon of alanine to obtain quasi-isosteric analogues of naturally occurring fluorescent amino acids.

Keywords: Benzo[*b*]thiophene derivatives; Fluorescent amino acids; Intramolecular charge transfer; Tryptophan analogues

1. Introduction

Thiophene-based compounds have recently renewed interest in their electronic and photophysical properties, inspiring both intense research activity [1,2] and technological applications, as in the case of polythiophenes in the design of optoelectronic devices [3,4]. In particular, benzo[*b*]thiophene (BT) derivatives revealed interesting bioactive properties of pharmacological and medical concern, showing antihyperglycemic activity as inhibitors of protein tyrosine phosphatase [5] or T-cell suppressor ability in patients affected by myelopathy spastic paresis [6].

Fluorescent peptides are commonly used for probing biological structure, function and interactions [7]. Alterations in emission band position, fluorescence time decay, quantum yield or polarization have been all exploited to detect and characterize biochemical processes [8]. Charge transfer (CT) probes have been frequently employed because of the high sensitivity of their fluorescence properties to the local polarity of the environment. Synthetic fluorescent amino acids with a strong CT character have been used to probe the strength of electrostatic interactions within the protein [9]. Unfortunately, the interpretation of protein fluorescence or peptide/protein interaction by fluorescence methods is often complicated by the presence of several tryptophan and tyrosine residues. A suitable approach is represented by the synthesis of new fluorescent analogues with excitation and emission properties well separated from those of naturally occurring amino acids [10]. Quasi-isosteric replacement of the indole nucleus by BT-based fluorophores has been achieved in a series of compounds of pharmacological interest [11,12].

In the present paper, we characterize the fluorescence properties of the BT derivatives reported in Fig. 1. The BT-based compounds differ in the type and position of the substituents: in position 3, a phenyl group (PhBT) or 4-methylsulfanylphenyl (SPhBT) and in position 7 an aminophenyl group (PhNBT) or an amino-(4-methyl-

* Corresponding author. Tel.: +39 06 72594468; fax: +39 06 72594328.
E-mail address: venanzi@uniroma2.it (M. Venanzi).

1010-6030/$ – see front matter © 2004 Elsevier B.V. All rights reserved.
doi:10.1016/j.jphotochem.2004.08.011

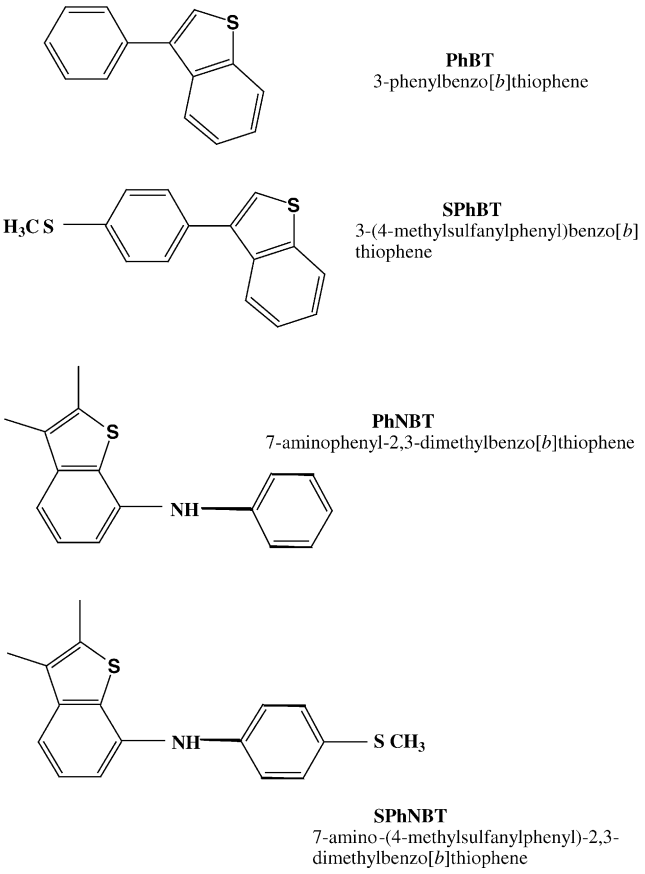

Fig. 1. Molecular formulae and acronyms of the synthesized benzo[*b*]-thiophene derivatives.

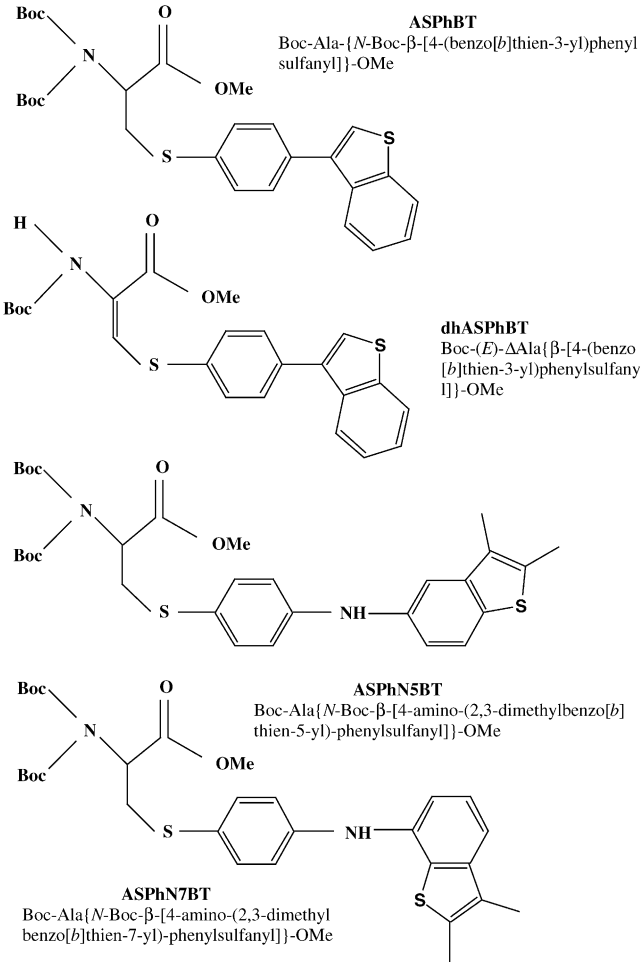

Fig. 2. Molecular formulae and acronyms of the synthesized benzo[*b*]-thienylamino acids.

sulfanyl)phenyl group (SPhNBT). Sulfanyl-substituted BT fluorophores were covalently linked to an amino acid template, giving rise to the new alanine derivatives reported in Fig. 2. In the amino acids, a sulfur atom in the *para* position bridges a 3-phenylbenzo[*b*]thiophene moiety to an alanyl scaffold in ASPhBT, a 5-aminophenylbenzo[*b*]thiophene in ASPhN5BT and a 7-aminophenylbenzo[*b*]thiophene in ASPhN7BT. Interesting photophysical effects were observed, where the 3-phenylbenzo[*b*]thiophene moiety is linked through the sulfur atom to a dehydroalanine scaffold (dhASPhBT). Dehydroamino acids are biologically active compounds, with important applications in structure–activity studies due to the high conformational constraints they impose [13].

2. Experimental

2.1. Materials

Acronyms of the compounds investigated are as follows: PhBT = 3-phenylbenzo[*b*]thiophene; SPhBT = 3-(4-methylsulfanylphenyl)benzo[*b*]thiophene; PhNBT = 7-aminophenyl-2,3-dimethylbenzo[*b*]thiophene; SPhNBT = 7-amino-(4-methylsulfanylphenyl)-2,3-dimethylbenzo[*b*]thiophene; ASPhBT = Boc-Ala-{*N*-Boc-β-[4-(benzo[*b*]thien-3-yl)phenylsulfanyl]}-OMe; dhASPhBT = Boc-(*E*)-ΔAla{β-[4-(benzo[*b*]thien-3-yl)phenylsulfanyl]}-OMe; ASPhN5BT = Boc-Ala{*N*-Boc-β-[4-amino-(2,3-dimethylbenzo[*b*]thien-5-yl)-phenylsulfanyl]}-OMe; ASPhN7BT = Boc-Ala{*N*-Boc-β-[4-amino-(2,3-dimethylbenzo[*b*]thien-7-yl)-phenylsulfanyl]}-OMe. BOC = *tert*-butoxycarbonyl.

The synthesis of compounds ASPhBT, dhASPhBT, ASPhN5BT and ASPhN7BT was already reported elsewhere [14].

2.1.1. Synthesis of compounds PhBT and SPhBT by C–C palladium catalysed cross-couplings

2.1.1.1. General procedure. To a solution of the brominated compound (0.05 M) in DME (dimethoxyethane)/H_2O (10:1), 3-benzo[*b*]thienylboronic acid (1.3 equiv.), $Pd(PPh_3)_4$ (10 mol%), Na_2CO_3 (2 equiv.) were added and the mixture was heated at 90 °C being the reaction monitored by TLC. The DME was removed under reduced pressure and the residue was dissolved in ethyl acetate (15 mL). The organic layer was then washed with water and brine (2 × 5 mL),

dried with $MgSO_4$ and the solvents were evaporated at reduced pressure.

2.1.1.2. PhBT. The procedure described above was applied using bromobenzene (0.50 mmol, 0.053 mL) and heating for 1 h. Column chromatography using petroleum ether gave compound PhBT (0.068 g, 65%) as a colourless oil. ^{1}H NMR (300 MHz, $CDCl_3$): δ 7.39–7.44 (m, 4H, ArH), 7.45–7.53 (m, 2H, ArH), 7.59–7.63 (m, 2H, ArH), 7.92–7.96 (m, 2H, ArH) ppm. ^{13}C NMR (75.4 MHz, $CDCl_3$): δ 122.91 (CH), 123.39 (CH), 124.31 (CH), 124.39 (CH), 127.53 (CH), 128.70 (CH), 128.71 (CH), 136.00 (C), 137.89 (C), 138.08 (C), 140.67 (C) ppm. MS (IE): *m/z* (%) = 212 (7) [M^+ + 2], 211 (17) [M^+ + 1], 210 (100) [M^+], 209 (19) [$M^+ - 1$], 208 (15) [$M^+ - 2$], 178 (9) [$M^+ - 32$], 165 (30) [$M^+ - 45$]. HRMS Calcd. for $C_{14}H_{10}S$ [M^+] 210.0503; found 210.0496.

2.1.1.3. SPhBT. The procedure described above was applied using 4-bromothioanisol (2.0 mmol, 406 mg) and heating for 3 h. Column chromatography using a solvent gradient from neat petroleum ether to 10% diethyl ether in petroleum ether gave compound SPhBT (0.287 g, 56%) as a white solid. Crystallization from petroleum ether gave colourless crystals, m.p. 67.8–68.5 °C. ^{1}H NMR (300 MHz, $CDCl_3$): δ 2.56 (s, 3H, CH_3), 7.36–7.42 (m, 5H, ArH), 7.53 (d, 2H, J = 8.7 Hz, ArH), 7.89–7.94 (m, 2H, ArH) ppm. ^{13}C NMR (75.4 MHz, $CDCl_3$): δ 15.73 (CH_3), 122.73 (CH), 122.88 (CH), 123.15 (CH), 124.28 (CH), 124.36 (CH), 126.67 (CH), 128.97 (CH), 132.66 (C), 137.36 (C), 137.71 (C), 137.79 (C), 140.61 (C) ppm. $C_{15}H_{12}S_2$ (256.38): Calcd. C 70.27, H 4.72, S 25.01; found C 70.49, H 4.88, S 25.13.

2.1.2. Synthesis of compounds PhNBT and SPhNBT by C–N palladium-catalysed cross-couplings

2.1.2.1. General procedure. A dried Schlenk tube was charged under Ar with dry toluene (2 mL), the bromo compound was added and the mixture was heated for 10 min at 80 °C. $Pd(OAc)_2$ (10 mol%), BINAP (2,2′-bis(diphenylphosphino)-1,1′-binaphthyl,15 mol%) and Cs_2CO_3 (1.4 equiv.) were added and the mixture was heated for another 10 min at 80 °C. The amino compound was added in dry toluene (2 mL) and the mixture was heated with stirring at 100 °C under Ar for 20 h. Water and diethyl ether were added and the phases were separated. The aqueous phase was washed with diethyl ether (3 × 10 mL) and the organic phases were collected, dried ($MgSO_4$), filtered and the solvent was removed to give a brownish oil, which was submitted to column chromatography. Solvent gradient from neat petroleum ether to 20% diethyl ether/petroleum ether was used.

2.1.2.2. PhNBT. The procedure described above was followed using bromobenzene (1.0 mmol, 0.105 mL) and 7-amino-2,3-dimethyl-benzo[*b*]thiophene (1 mmol, 0.177 mg). Column chromatography gave PhNBT (0.153 g, 61%) as a white solid, m.p. 91.1–91.6 °C. ^{1}H NMR (300 MHz, $CDCl_3$): δ 2.32 (s, 3H, $ArCH_3$), 2.50 (s, 3H, $ArCH_3$), 5.60 (s broad, 1H, NH), 6.93–6.99 (m, 1H, ArH), 7.05–7.08 (m, 2H, ArH), 7.16–7.21 (m, 1H, ArH), 7.26–7.32 (m, 4H, ArH). ^{13}C NMR (75.4 MHz, $CDCl_3$): δ 11.65 (CH_3), 13.84 (CH_3), 112.65 (CH), 115.36 (CH), 117.88 (CH), 120.95 (CH), 124.94 (CH), 128.16 (C), 129.23 (CH), 129.54 (C), 133.00 (C), 137.17 (C), 142.66 (C), 143.04 (C) ppm. $C_{16}H_{15}NS$ (253.36): Calcd. C 75.85, H 5.97, N 5.53, S 12.65; found C 75.71, H 6.13, N 5.43, S 12.51.

2.1.2.3. SPhNBT. The procedure described above was followed using 4-methylsulfanylaniline (0.5 mmol, 0.043 mL) and 7-bromobenzo[*b*]thiophene (0.5 mmol, 0.121 g). Column chromatography gave compound SPhNBT (0.060 g, 40%) as an oil. Crystallization from diethyl ether/petroleum ether gave light yellow crystals, m.p. 130.0–131.7 °C. ^{1}H NMR (300 MHz, $CDCl_3$): δ 2.32 (s, 3H, CH_3), 2.48 (s, 3H, CH_3), 2.50 (s, 3H, CH_3), 5.60 (s broad, 1H, NH), 7.00 (d, 2H, J = 8.7 Hz, ArH), 7.11–7.16 (m, 1H, ArH), 7.26 (d, 2H, J = 8.7 Hz, ArH), 7.27–7.31 (m, 2H, ArH). ^{13}C NMR (75.4 MHz, $CDCl_3$): δ 11.63 (CH_3), 13.83 (CH_3), 17.82 (SCH_3), 112.70 (CH), 115.47 (CH), 118.57 (CH), 124.94 (CH), 128.15 (C), 128.97 (C), 129.51 (C), 129.71 (CH), 133.06 (C), 137.01 (C), 141.29 (C), 142.68 (C) ppm. $C_{17}H_{17}NS_2$ (299.45): Calcd. C 68.19, H 5.72, N 4.68, S 21.41; found C 68.20, H 6.07, N 4.58, S 21.13.

Solvents used for spectroscopic studies were all spectroscopic grade (Carlo Erba, Italy). Abbreviations: methanol (MeOH), acetonitrile (MeCN), propanol-2 (i-PrOH), hexane (Hex), dioxane (Diox).

2.2. Methods

Steady-state fluorescence spectra were recorded on a Fluoromax spectrofluorimeter (Jobin-Yvon, France), operating in SPC (single photon counting) mode. Quantum yields were obtained by using naphthalene in cyclohexane as reference: $\phi_0 = 0.23 \pm 0.02$ [15]. Nanosecond time decays were measured by a CD900 lifetime apparatus with SPC detection (Edinburgh Instruments, UK). Excitation in the UV region was achieved by a flashlamp filled with ultrapure hydrogen (0.3 bar), working at a repetition rate of 30 kHz. Experimental decay curves were fitted by a nonlinear least-squares analysis to exponential functions by using standard software licensed by Edinburgh Instruments. All fluorescence experiments were carried out in quartz cells, using solutions previously bubbled for 20 min with ultrapure nitrogen.

Theoretical calculations were performed by obtaining the most stable conformations of the molecules in acetonitrile solutions via molecular mechanics calculations. Solvent effects were accounted for by introducing in the electrostatic term of the potential energy function the corresponding bulk dielectric constant [16]. The SPARTAN program was used to find the electronic energies and distributions associated to the most stable conformers by ab initio RHF methods, using a STO 31G** basis set [17].

3. Results and discussion

3.1. Benzo[b]thiophene derivatives: PhBT, SPhBT, PhNBT, SPhNBT

3.1.1. Absorption experiments

The UV spectral features of benzo[*b*]thiophene are characterized by two absorption bands in the 230–250 nm ($\pi \rightarrow \pi^*$, ^{1}B transition, $\log \varepsilon$ = 3.7–4.8) and 270–320 nm ($\pi \rightarrow \pi^*$, ^1L_a and ^1L_b transitions, $\log \varepsilon$ = 3.1–4.5) wavelength regions [18]. Following the assignments made by Meech et al. [19] on the absorption bands of the analogous indole chromophore, the longer wavelength band (300–330 nm) can be ascribed to the ^1L_b transition and the absorption between 270 and 300 nm to the ^1L_a transition. It was observed that the whole BT low-energy band system, spanning between 220 and 325 nm, is unaffected in energy position when the solvent polarity is largely changed on going from *n*-heptane (ε_s = 1.9) to acetonitrile (ε_s = 37.5) [20].

The data reported in Table 1 and the absorption spectra shown in Fig. 3 for PhBT and SPhBT in acetonitrile reveal that the alkylsulfanyl substitution only slightly perturbs the absorption spectral features of the phenylbenzothiophene chromophore. Larger effects are measured in the case of the phenylaminobenzo[*b*]thiophene compounds, the lowest energy (LE) transitions of SPhNBT being markedly shifted to longer wavelengths with respect to PhNBT, as clearly shown by the absorption spectra in acetonitrile reported in Fig. 4. The presence in the same molecular frame of an electron-rich sulfanyl group (MeS–), interacting through a phenyl moiety with a strong electron-donor substituent (–NH–) directly linked to benzo[*b*]thiophene, capable to fulfil both electron-accepting or -donating functions, markedly affects the LE Franck–Condon transition of the substituted BT chromophore. The electronic coupling between a dimethylamino group and the thiophene units of derivatized oligothiophenes has been exploited in the design of push-pull chromophores [21]. The charge-transfer process, originated from the dimethylamino group and propagated through the π-conjugated spacers, gives rise to a considerable bathochromic shift of the thiophene transitions. This effect is associated to a dramatic enhancement of the nonlinear optical properties of the oligomer [21]. A red shift of the LE transition of diphenylsulfide was also observed when an amino group substituted one of the phenyl units at the *para* position [22]. In this case, the formation of a highly dipolar quinoid mesomeric structure was made possible by the π-conjugation of the two phenyl groups through the sulfide bridge. These results suggest that the sulfanylphenyl group in SPhNBT participate to the stabilization of charge-transfer intramolecular interactions from the amino group to benzothiophene.

Table 1
Absorption (λ_{max}(Abs)) and emission (λ_{max}(Em)) maximum wavelengths, and fluorescence quantum yield (Φ) in acetonitrile

Sample	λ_{max}(Abs) (nm)	λ_{max}(Em) (nm)	Φ[a]
PhBT	302, 293, 262, 231	337	0.02
SPhBT	303, 293,276, 234	365	0.05
PhNBT	293, 262, 230	364	0.01
SPhNBT	302, 269, 230	413	0.03
ASPhBT	303, 277, 231	356	0.08
dhASPhBT	306, 230	408	<0.001
ASPhN7BT	303, 269, 230	390	0.02
ASPhN5BT	305, 280, 230	395	0.01

[a] With respect to naphthalene in cyclohexane (Φ_0 = 0.23).

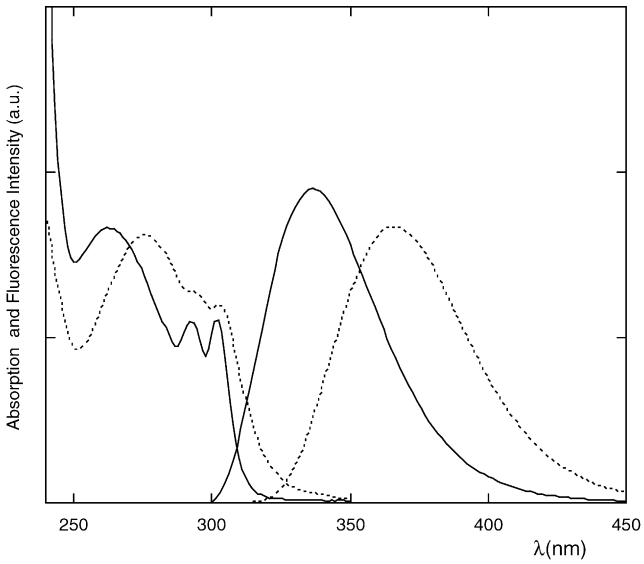

Fig. 3. Absorption and fluorescence spectra of PhBT (continuous lines) and SPhBT (dotted lines) in acetonitrile. Absorption spectra are normalized with respect to the lowest energy absorption maximum. Fluorescence spectra are normalized to unit area.

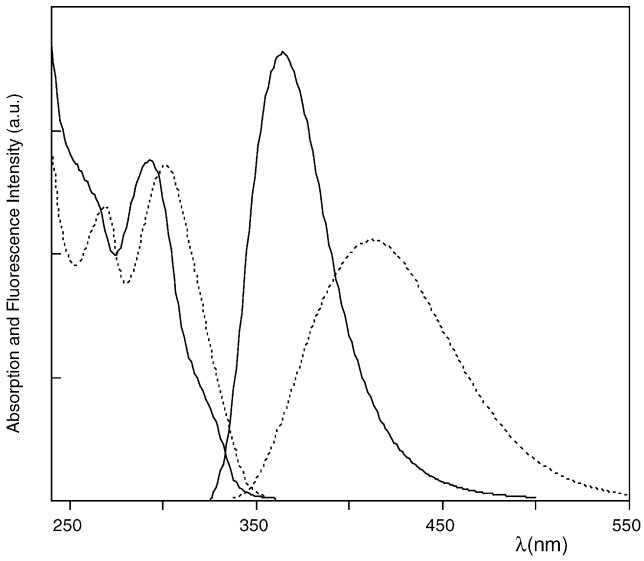

Fig. 4. Absorption and fluorescence spectra of PhNBT (continuous lines) and SPhNBT (dotted lines) in acetonitrile. The absorption spectra are normalized with respect to the lowest energy absorption maximum. Fluorescence spectra are normalized to unit area.

Table 2
Fluorescence time decay (τ), radiative (k_r) and non-radiative (k_{nr}) rate constants in acetonitrile

Sample	τ (ns)	k_r (10^{-8} s^{-1})	k_{nr} (10^{-9} s^{-1})
PhBT	0.17	1.2	5.8
SPhBT	0.36	1.4	2.6
PhNBT	0.30	0.3	3.3
SPhNBT	1.47	0.2	0.7
ASPhBT	0.35	2.3	2.6
ASPhN7BT	0.88	0.2	1.1
ASPhN5BT	0.68	0.1	1.4

3.1.2. Steady-state and time-resolved fluorescence experiments

The fluorescence properties of benzo[*b*]thiophene were measured in ethanol at 77 K, showing a 0–0 emission band at 304 nm and emission quantum yields comprised between 0.035 and 0.02 [23,24]. The fluorescence spectra of PhBT and SPhBT in acetonitrile at room temperature (Fig. 3) show a single band peaked at 337 and 362 nm, respectively. The alkylsulfanyl substitution on the phenyl group deeply affects the photophysics of the phenylbenzo[*b*]thiophene fluorophore, as can be evinced by the data reported in Table 1 for steady-state and Table 2 for time-resolved fluorescence measurements in acetonitrile: (i) the SPhBT emission spectrum shifts to longer wavelengths by 25 nm, corresponding to lower the S_1–S_0 energy gap by 0.26 eV; (ii) the SPhBT quantum yield doubles the quantum yield of PhBT and (iii) the SPhBT time decay parallels the quantum yield increase.

Radiative (k_r) and non-radiative (k_{nr}) rate constants can be obtained from the measured quantum yield and time decay by the following equation:

$$k_r = \frac{\Phi}{\tau}, \qquad k_{nr} = \frac{1}{\tau} - k_r \tag{1}$$

where k_{nr} denotes the sum of the rate constants associated to the different radiationless processes (internal conversion, intersystem crossing, intramolecular charge transfer, etc.). From the rate constants values, also reported in Table 2, it clearly appears that the alkylsulfanyl substitution strongly decreases the efficiency of the non-radiative processes, letting almost unchanged the corresponding radiative rate constants. The photophysics of benzothiophene is dominated by the triplet formation quantum yield (Φ_T=0.98) [24], as confirmed by the large values of the non-radiative rate constants in Table 2. The alkylsulfanyl substitution perturbs the excited-state electronic distribution of benzothiophene, decreasing the efficiency of the intersystem crossing to the triplet state and shifting the emission to longer wavelengths. This finding suggests the contribution of polar structures to the SPhBT excited state, favoured by partial electronic delocalization from the sulfanylphenyl group to the benzo[*b*]thiophene moiety.

The same effects induced by the alkylsulfanyl substitution on PhBT, i.e. red-shifted emission, increased fluorescence quantum yield and lifetime, unchanged radiative rate constant and decreased non-radiative rate constant, are observed in the case of the aminobenzo[*b*]thiophene derivatives (Tables 1 and 2, Fig. 4). The introduction of an electron–donor NH group bridging the phenyl and the BT aromatic moieties, gives rise to interesting differences in the photophysical properties of PhNBT and SPhNBT, that can be characterized by measuring their absorption and emission spectral features in solvents of different polarity. The experimental results can be described in terms of the Lippert–Mataga equation, relating the energy difference between the absorption and emission maxima to the different orientation polarizability of the fluorophore (Δf) in a given solvent [8]:

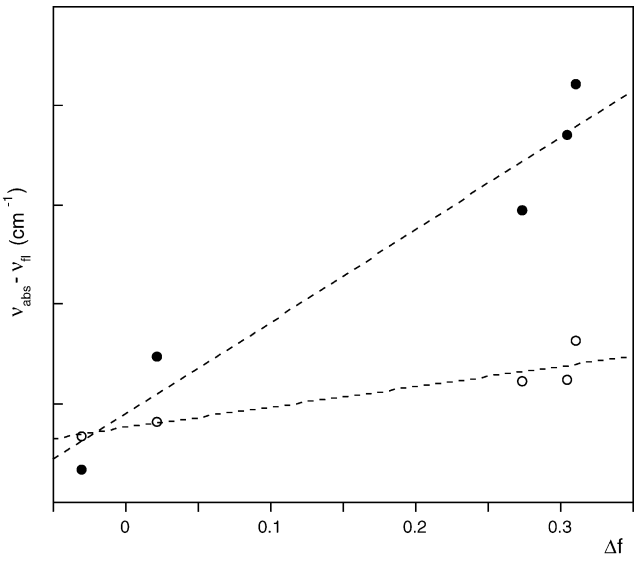

Fig. 5. Difference between the absorption and emission maxima (wavenumbers) vs. the orientation polarizability (Δf) of different solvents (Hex: Δf = −0.0312; Diox: 0.0205; i-PrOH: 0.273; MeOH: 0.304; MeCN: 0.310). Full circles: SPhNBT; empty circles: PhNBT.

$$\bar{\nu}_A - \bar{\nu}_F = \frac{2(\mu_E - \mu_G)^2}{hca^3}\Delta f + \text{constant} \tag{2}$$

In Eq. (2), μ_G and μ_E represent the ground- and excited-state dipole moments, respectively, and a the radius of the cavity hosting the fluorophore. Δf can be approximately obtained by the static dielectric constant (ε) and refractive index (n) of the bulk solvent:

$$\Delta f = \frac{\varepsilon - 1}{2\varepsilon + 1} - \frac{n^2 - 1}{2n^2 + 1} \tag{3}$$

The corresponding Lippert–Mataga plot ($\bar{\nu}_{abs} - \bar{\nu}_{fl}$ versus Δf), shown in Fig. 5, exhibits a fairly linear correlation for both compounds, with similar intercepts, but very different slopes (9339 cm^{-1} for SPhNBT and 2174 cm^{-1} for PhNBT). From theoretical calculations, we estimated the cavity radius a and the ground-state dipole moment μ_G for PhNBT (a = 3.7 Å; μ_G = 2.60 Da) and SPhNBT (a = 3.9 Å; μ_G = 2.91 Da). From these computed quantities and the experimental results reported in Fig. 5, we obtained the excited-state dipole moment for PhNBT (μ_E = 5.1 Da) and SPhNBT (μ_E = 10.3 Da). The latter μ_E value is typical of planar S_1 (π^*)

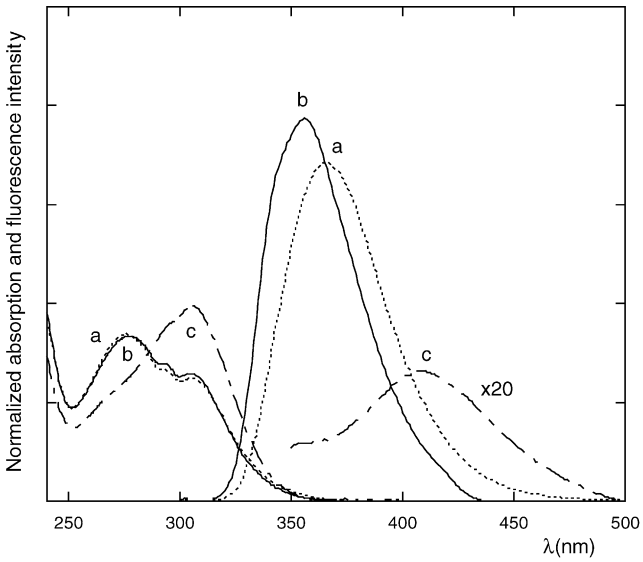

Fig. 6. Absorption and emission spectra of SPhBT (a, dotted lines), ASPhBT (b, continuous lines) and dhASPhNBT (c, dashed-dotted lines) in acetonitrile. The fluorescence spectrum of dhASPhNBT is multiplied by a factor 20 for clarity. The absorption spectra are normalized with respect to the lowest energy absorption maximum. Fluorescence spectra (a,b) are normalized to unit area.

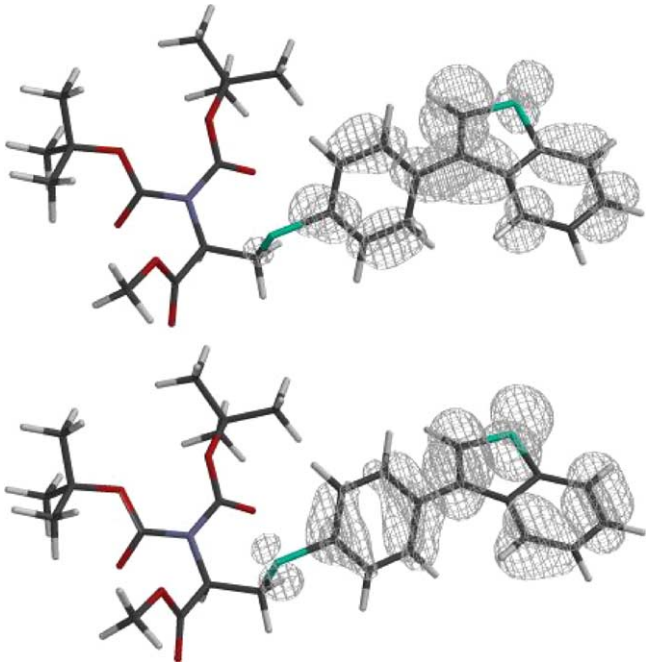

Fig. 7. LUMO (upper) and HOMO (lower) electronic wavefunctions of ASPhBT.

state with partial contributions of polar structures, giving rise to planar intramolecular charge transfer (PICT) states [25]. Twisted intramolecular charge-transfer (TICT) states, usually detected in secondary aromatic amines, generally show much higher excited-state dipole moments (20–30 Da). These findings suggest that planar quinoid mesomeric structures, made possible by the delocalization of the sulfanyl electronic distribution through the phenyl group, contribute to increase the polar character of the SPhNBT excited state.

3.2. Benzo[b]thienylalanine derivatives: ASPhBT, dhASPhBT, ASPhN7BT, ASPhN5BT compounds

3.2.1. ASPhBT and dhASPhBT

The linkage of SPhBT to alanine does not perturb the ground-state electronic properties of the benzo[*b*]thiophene chromophore, as shown by the fine overlap of the absorption spectra of ASPhBT and SPhBT in acetonitrile reported in Fig. 6. On the contrary, the benzothiophene emission in ASPhBT is shifted to shorter wavelengths by 9 nm with respect to the SPhBT emission, while its fluorescence quantum yield remarkably increases (Table 1). By comparing the photophysical rate constants of the two compounds (Table 2), it appears that the inclusion in the amino acid scaffold does not affect the efficiency of the intramolecular quenching processes, but increases the radiative rate constant. These findings suggest that the linkage to the amino acid weakens the excited-state electronic coupling between the phenylsulfanyl group and the benzo[*b*]thiophene fluorophore, decreasing the weight of charge-transfer contributions to the excited state of ASPhBT.

The optical properties of ASPhBT are strongly perturbed by dehydrogenating the alanine C^{α}–C^{β} bond. The LE absorption band of the dehydrogenated amino acid dhASPhBT appears to be significantly red-shifted and structureless (Fig. 6), suggesting a large delocalization of the BT electronic distribution over the entire molecular scaffold. Furthermore, the fluorescence emission of dhASPhBT is almost completely quenched and the barely detectable band, centered at 411 nm, is shifted by more than 50 nm with respect to the ASPhBT emission in acetonitrile (Fig. 6).

Quantum mechanical calculations were performed on ASPhBT and dhASPhBT to investigate the ground- and excited-state electronic properties of the two compounds. Figs. 7 and 8 report the HOMO and LUMO wavefunctions of ASPhBT and dhASPhBT, respectively. It clearly appears that both the ground and excited states of the former compound are localized on the phenylbenzo[*b*]thiophene moiety, while in the dehydrogenated amino acid the HOMO and, with a greater extent, the LUMO electronic distributions are largely delocalized through the amino acid backbone. Most likely, the electronic coupling of the BT chromophore to the dehydroalanine residue opens non-radiative relaxation channels, that almost completely deplete the fluorescence emission.

3.2.2. Probing the electronic conjugation through the amino acid side chain: ASPhN7BT and ASPhN5BT compounds

The charge-transfer interaction revealed in the case of SPhNBT can be usefully exploited to probe the degree of electronic conjugation of the BT chromophore to the amino acid scaffold. As clearly shown in Fig. 9, the absorption spec-

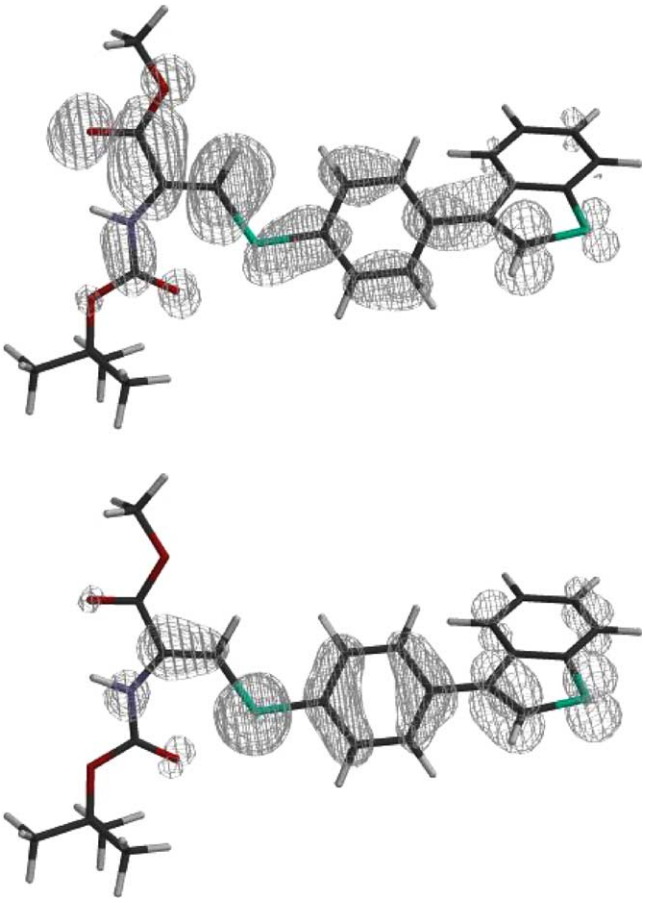

Fig. 8. LUMO (upper) and HOMO (lower) electronic wavefunctions of dhASPhBT.

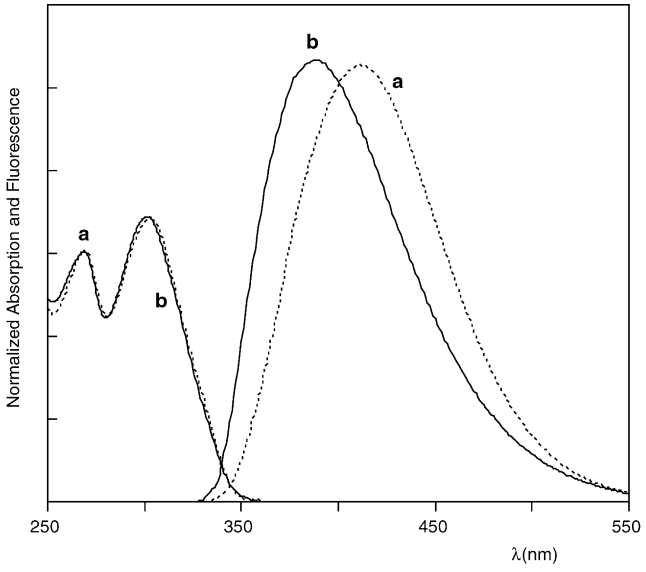

Fig. 9. Absorption and emission spectra of SPhNBT (a, dotted lines), ASPhN7BT (b, continuous lines) in acetonitrile. The absorption spectra are normalized with respect to the lowest energy absorption maximum. Fluorescence spectra are normalized to unit area.

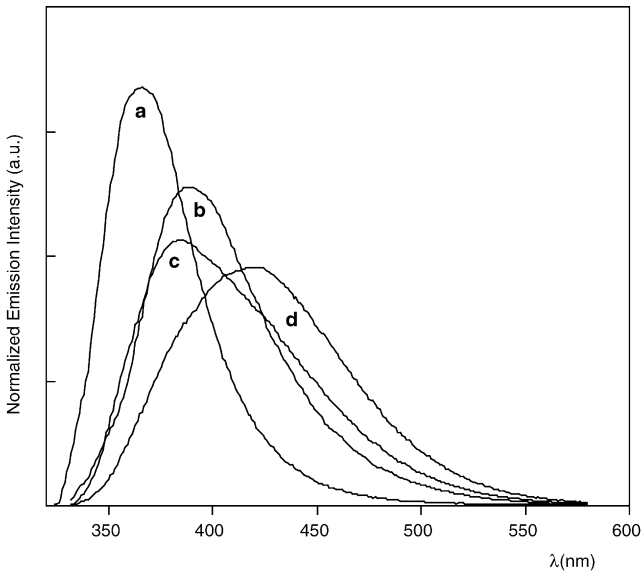

Fig. 10. Fluorescence spectra in methanol of PhNBT (a), ASPhN5BT (b), ASPhN7BT (c) and SPhNBT (d). Fluorescence spectra are all normalized to unit area.

trum of ASPhN7BT is not perturbed by linking the aminobenzothiophene group to the amino acid side chain, in contrast with the relaxed excited state responsible for the fluorescence emission. Since solvent relaxation effects are determined by the fluorophore excited-state polarity, the significant blue shift of the ASPhN7BT emission in acetonitrile, indicates a minor CT contribution to its excited state with respect to the SPhNBT compound. The possibility to use solvent effects to characterize the polarity and, hence, the weight of CT contributions to the excited state electronic distribution of BT-based compounds, is clearly demonstrated in Fig. 10, where we report the fluorescence spectra in methanol of PhNBT (smallest contribution of CT interaction, λ_{max} = 366 nm), SPhNBT (maximum CT interaction, λ_{max} = 421 nm) and of the two alanine-BT derivatives ASPhN7BT (λ_{max} = 384 nm) and ASPhN5BT (λ_{max} = 386 nm). The latter compounds differ only in the position of the amino substituent on the benzo[*b*]thiophene ring (Fig. 2). The substitution pattern affects the BT electronic distribution and, consequently, the delocalization through the amino acid scaffold and the extent of CT interactions. Remarkably, the width of the emission band increases on going from PhNBT to SPhNBT, denoting that the interaction between the solvent molecules and the chromophore excited state gives rise to an heterogeneous population of fluorophores characterized by a continuous distribution of relaxed states. The linkage to the amino acid scaffold perturbs the excited-state electronic distribution of the BT-based derivatives, reducing the extent of the intramolecular CT interaction propagated through the phenylsulfanyl and the amino groups. Accordingly, the non-radiative rate constants of ASPhN7BT and ASPhN5BT show intermediate values with respect to those measured for PhNBT and SPhNBT (Table 2). The chemical motif determining

the photophysics of the compounds investigated is the electronic coupling of the sulfanyl group to the amino acid residue and the extent of the CT interaction within the sulfanyl/phenyl/aminobenzo[*b*]thiophene moiety.

4. Conclusions

Benzo[*b*]thiophene demonstrates a molecular scaffold featuring optical properties capable of interesting applications: (i) it is easily endowed with different chemical functions and (ii) its spectroscopic properties can be modulated by proper substitution on the aromatic ring. The delicate balance between the delocalization of the aromatic electronic distribution through the molecular frame and the extent of intramolecular charge-transfer interactions in the ground and excited electronic states can be controlled by careful selection of the nature and position of the BT substituents. As a result, the excitation and emission energy range of the chromophore and its sensitivity to the chemical environment polarity can be suitably tuned.

We explored the possibility to use BT-based compounds as synthetic analogues of naturally occurring fluorescent amino acids by covalently linking several sulfanyl-substituted BT derivatives to the side chain of alanine. It is shown that it is possible to control the emission properties of the probe by varying the linkage to the amino acid side chain. This finding could be usefully exploited to switch on (off) the signal of BT-based fluorophores by hydrogenating (dehydrogenating) the amino acid side chain. These properties make benzo[*b*]thiophene and its derivatives valuable building blocks in the design and synthesis of multifunctional supramolecular architectures based on peptide units [26].

References

[1] Y. Shiroda, M. Kinoshita, T. Noda, K. Okumoto, T. Ohara, J. Am., Chem. Soc. 122 (2000) 11021–11022.
[2] Y. Yokoyama, H. Shiraishi, Y. Tani, Y. Yokoyama, Y. Yamagushi, J. Am. Chem. Soc. 125 (2003) 7194–7195.
[3] M.R. Andersson, O. Thomas, M. Svensson, M. Theander, O. Ingänas, J. Mater. Chemistry 9 (1999) 1933–1940.
[4] B.L. Grönendaal, F. Jonasa, D. Freitag, H. Pielarrtzik, J.R. Reynolds, Adv. Mater. 12 (2000) 481–494.
[5] M.S. Malamas, J. Sredy, C. Moxham, A. Katz, W.X. Xu, R. McDevitt, F.O. Adebayo, D.R. Sawicki, L. Seestaller, D. Sullivan, J.R. Taylor, J. Med. Chem. 43 (2000) 1293–1310.
[6] M. Makino, M. Azuma, S.I. Wakamatsu, Y. Suruga, S. Izumo, M.M. Yokohama, M. Baba, Clin. Diagn. Lab. Immunol. 6 (1999) 316–322.
[7] B. Pispisa, C. Mazzuca, A. Palleschi, L. Stella, M. Venanzi, F. Formaggio, C. Toniolo, J.-P. Mazaleyrat, M. Wakselman, J. Fluorescence 13 (2003) 139–147.
[8] J.R. Lakowicz, Principles of Fluorescence Spectroscopy, Kluwer Academic Publishers, New York, 1999.
[9] J.J. La Clair, Angew. Chem. Int. Ed. Engl. 37 (1998) 325–329.
[10] B.E. Cohen, T.B. McAnaney, E.S. Park, Y.N. Jan, S.G. Boxer, L.Y. Jan, Science 296 (2002) 1700–1703.
[11] T.P. Blackburn, D.T. Davies, I.T. Forbes, C.J. Hayward, C.N. Johnson, R.T. Martin, D.C. Piper, D.R. Thomas, M. Thompson, N. Upton, R.W. Ward, Bioorg. Med. Chem. Lett. 5 (1995) 2589–2592.
[12] F. Da Settimo, A. Lucacchini, A.M. Marini, C. Martini, G. Primofiore, G. Senatore, S. Taliani, Eur. J. Med. Chem. 31 (1996) 951–956.
[13] A. Giannis, T. Kolter, Angew. Chem. Int. Ed. Engl. 32 (1993) 1244–1247.
[14] A.S. Abreu, N.O. Silva, P.M.T. Ferreira, M.J.R.P. Queiroz, Eur. J. Org. Chem. (2003) 1537–1544.
[15] D.F. Eaton, Pure Appl. Chem. 60 (1988) 1107–1144.
[16] B. Pispisa, A. Palleschi, L. Stella, M. Venanzi, C. Toniolo, J. Phys. Chem. B 102 (1998) 7890–7898.
[17] Spartan Version 4.0, Washington, Inc., Irvine, CA, 1998.
[18] J.J. Aaron, Z. Mechbal, A. Adenier, C. Parkanyi, V. Kozmic, J. Svoboda, J. Fluorescence 12 (2002) 231–239.
[19] S.R. Meech, D. Phillips, A.G. Lee, Chem. Phys. 80 (1983) 317–328.
[20] T. Misra, T. Ganguly, S. Kamila, C. Basu, A. De, Spectrosc. Acta A 57 (2001) 2795–2808.
[21] J.M. Raimundo, P. Blanchard, N. Gallego-Planas, N. Mercier, I. Ladoux-Rak, R. Hierle, J. Roncali, J. Org. Chem. 67 (2002) 205–218.
[22] D.B. O'Connor, G.W. Scott, K. Tran, D.R. Coulter, V.M. Minkowski, A.E. Stiegman, G.E. Wnek, J. Chem. Phys. 97 (1992) 4018–4028.
[23] M. Zander, Z. Naturforsch. 40A (1985) 497–502;
M. Zander, G. Kirsch, Z. Naturforsch. 44A (1989) 205–209.
[24] S. Murov, I. Carmichael, G.L. Hug, Handbook of Photochemistry, 2nd ed., Marcel Dekker, New York, 1993.
[25] Z.R. Grabowski, K. Rotkiewicz, W. Rettig, Chem. Rev. 103 (2003) 3899–4031.
[26] M. Venanzi, A. Palleschi, L. Stella, B. Pispisa, in: L. Barsanti, V. Evangelista, P. Gualtieri, V. Passarelli, S. Vestri (Eds.), Molecular Electronics: Bio-sensors and Bio-computers, Kluwer Academic Publishers, Dordrecht, 2003, pp. 237–254.